Violation of classical inequalities by frequency-filtering

C. Sánchez Muñoz, E. del Valle, C. Tejedor, and F.P. Laussy*
Departamento de Física Teórica de la Materia Condensada and Condensed Matter Physics Center (IFIMAC), Universidad Autónoma de Madrid, E-28049, Spain.
(Dated: March 26, 2014)

The violation of the Cauchy–Schwarz and Bell inequalities ranks among the major evidences of the genuinely quantum nature of an emitter. We show that by dispensing from the usual approximation of mode correlations and studying directly correlations between the physical reality—the photons—these violations can be optimized. This is achieved by extending the concept of photon correlations to all frequencies in all the possible windows of detections, with no prejudice to the supposed origin of the photons. We identify the regions of quantum emission as rooted in collective de-excitation involving virtual states instead of, as previously assumed, cascaded transitions between real states.

PACS numbers: 42.50.Ct, 42.50.Ar, 42.50.Pq

arXiv:1403.6182v1 [quant-ph] 24 Mar 2014

Classical descriptions of the electromagnetic field [1] and local hidden variable theories [2] yield a series of inequalities that impose an upper limit to the correlations between two modes and whose violation prove unequivocally the non-classical character of quantum mechanics [3]. Among such equalities, the Cauchy–Schwarz inequality and Bell's inequalities are prominent examples that have been put to scrutiny in a large and varied set of platforms. The Cauchy–Schwarz Inequality (CSI) [4] is one of the most important relations in all of mathematics. It states that fluctuations of products of random variables are bounded by the product of autocorrelations: $|\langle XY\rangle| \leq \sqrt{\langle X^2\rangle\langle Y^2\rangle}$. When X and Y are quantum observables, however, this relation can be violated. That is to say, quantum correlations between two objects can be so strong as to overcome their individual fluctuations in a way that is unaccountable by classical physics. Bell's inequalities (BI), on the other hand, refer to the wider problem of the nonlocal character of quantum mechanics. Their violation decides in favour of quantum theory over local hidden variable theories. The underlying correlations are well known to power quantum information processing [5]. In a quantum optical context, these inequalities can be expressed through the correlators $\langle a_i^\dagger a_j^\dagger a_j a_i\rangle$, $\{i,j\} \in \{1,2\}$, of two bosonic modes a_1 and a_2. In terms of Glauber's second-order correlation functions at zero delay $g_{ij}^{(2)} = \langle a_i^\dagger a_j^\dagger a_j a_i\rangle / (\langle a_j^\dagger a_j\rangle\langle a_i^\dagger a_i\rangle)$ [6], the CSI reads $\left[g_{12}^{(2)}\right]^2 \leq g_{11}^{(2)} g_{22}^{(2)}$. This can be expressed in terms of a ratio R that quantifies the degree of CSI violation:

$$R = \left[g_{12}^{(2)}\right]^2 \Big/ \left[g_{11}^{(2)}\, g_{22}^{(2)}\right] . \qquad (1)$$

A two-mode Bell's inequality $B \leq 2$ can similarly be expressed in these terms, passing the photons through a beam splitter instead of preparing a quantum superposition [7][43], with:

$$B = \sqrt{2}\left|\frac{\langle a_1^{\dagger 2} a_1^2\rangle + \langle a_2^{\dagger 2} a_2^2\rangle - 4\langle a_1^\dagger a_2^\dagger a_2 a_1\rangle}{\langle a_1^{\dagger 2} a_1^2\rangle + \langle a_2^{\dagger 2} a_2^2\rangle + 2\langle a_1^\dagger a_2^\dagger a_2 a_1\rangle}\right| . \qquad (2)$$

These inequalities are violated when $R > 1$ and $B > 2$. The first experimental demonstrations were realized in the 70s in the radiation of an atomic two-photon cascade for the CSI [8] and in the early 80s for the BI [9–11]. There has been a large body of literature confirming and documenting such violations ever since [12–18] with reported values such as $R \approx 1.6$ [19], $R \approx 11\,600$ [20] or $R \approx 8.4 \times 10^6$ [21] for the CSI, and $B \approx 2.25$ [12], $B \approx 2.68$ [15] or $B \approx 2.83$ [16] for BI. Most experimental realizations in both cases involve the correlation of photons of different frequencies emitted in a multi-photon process, such as atomic cascades [9] or four-wave mixing [15, 21].

While in the underlying theoretical models these photons are attributed to quantum modes corresponding to specific optical transitions [3], the only physical reality perceived by the measuring devices are the photons themselves. One can therefore inquire what are the correlations between photons with a given property—for CSI and BI violation, typically their frequency—with no theoretical prejudice as to their origin. In this text, we address this question in a general context, but to fix ideas, we will illustrate our claims on one particular source of photons. To emphasize that the correlated photons do not need to be attached to different modes, we will consider a single-mode emitter. The simplest non-trivial candidate—resonance fluorescence—is also of great intrinsic interest and has been a favourite testbed of quantum optics [22]. It consists of the light emitted under strong coherent driving by a two-level system (2LS) [23–25]. At high pumping intensity, the luminescence spectrum splits into three peaks, known as the Mollow triplet [26] (cf. Fig. 1(a)). While the emission comes from a single mode, σ, the distinctive spectral shape calls naturally to question what are the correlations of—and between—the three peaks. It has been suggested theoretically [27–30] and established experimentally [29, 31, 32] that the photons from the peaks are strongly correlated. Recent results with semiconductor quantum dots [32] support that both Cauchy–Schwarz and Bell's inequal-

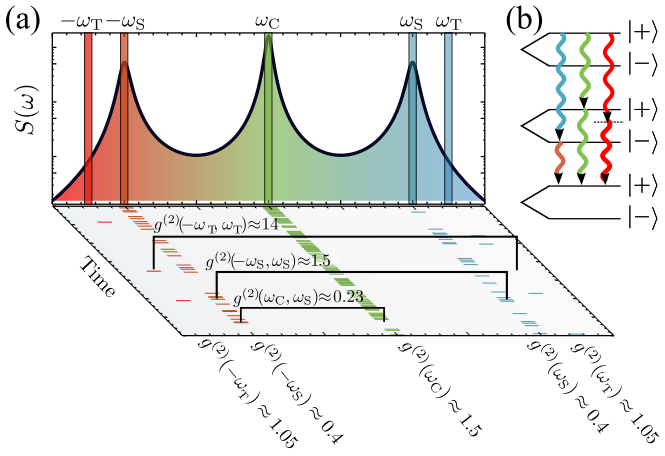

FIG. 1: (Color online) Violation of CSI and BI by frequency-resolved correlations. (a) Filtering illustrated in the tails (T), sidebands (S) and central peak (C) of the Mollow triplet. (b) Two-photon de-excitation between rungs of the Mollow ladder involve an intermediate real state or a virtual state. The latter type conveys CSI and BI violation. It is found in the flanks or between the peaks, where the signal is however weaker. Parameters: $\Omega = 10\gamma_\sigma$, $\Gamma = \gamma_\sigma$, $\omega_S = 2\Omega$, $\omega_T = 2.5\Omega$.

ities expressed in the form (1) and (2) have already been violated in resonance fluorescence, thought this was not explicitly pointed out by the authors.

The Hamiltonian for this system reads $H_0 = \omega_\sigma \sigma^\dagger\sigma + \Omega(e^{-i\omega_L t}\sigma^\dagger + e^{i\omega_L t}\sigma)$ with ω_σ the energy of the 2LS and Ω the intensity of the field driving it with frequency ω_L. With little loss of generality we will consider resonant excitation: $\omega_L = \omega_\sigma$. Dissipation is included in the Lindblad form with decay rate γ_σ for the emitter [33]. At this point, an ad hoc multiple-mode description is usually enforced out of the genuine single mode σ which, dressed by the laser, yields three types of transitions between the states $|\pm\rangle$ (cf. Fig. 1(b)). This allows to introduce three auxiliary modes, associated to the three peaks: $\sigma_1 = c^2|-\rangle\langle+|$, $\sigma_2 = cs\,[|+\rangle\langle+| - |-\rangle\langle-|]$ and $\sigma_3 = -s^2|+\rangle\langle-|$ with s and c two amplitudes [28, 30]. One can easily compute correlations $\langle\sigma_i^\dagger\sigma_j^\dagger\sigma_j\sigma_i\rangle$ for $1 \le i,j \le 3$ between these modes, that are associated in the input/output formalism [34] to those $\langle a_i^\dagger a_j^\dagger a_j a_i\rangle$ of the detected photons with a given frequency, allowing one to check whether Eqs. (1) and (2) violate their respective inequalities.

There are various shortcomings to this approach, which is an approximation rooted in the physical picture of the dressed atom. First, the identification of each photon to a given transition based on its frequency is a simplification. Although infrequent, it happens that a photon detected at the frequency of a given peak actually originates from the transition that chiefly accounts for another peak. When considering regions of overlap, such a misattribution can become a source of large errors. Second, this approach neglects interferences between photons that truly are emitted by the same mode σ. Third, modes defined in this way are usually non-commuting, and therefore correlations at zero delay can yield different results depending on the order of the operators [29]. Finally, this approach also restricts the calculation to the three modes thus defined, while one can correlate any two frequency windows, of various widths and centered at arbitrary frequencies, not compulsorily at the peak maxima.

To dispense from these approximations and constrains, an exact theory of frequency-resolved photon detection is required to correlate any two photons based only on their measured properties, with no assumption as to their origin or time of emission. The formal expression without recoursing to contrived modes has been formalized in the late 80s [35, 36]. It provides the statistics of photons with frequencies ω_1 and ω_2 spectrally filtered in a Lorentzian window of width Γ. We will denote it $g_\Gamma^{(2)}(\omega_1,\omega_2)$. The resulting integral form turns out to be so awkward, however, that even in the possession of the expression, there was the need to come back to the multi-mode approximation to compute it. In this text, we recourse to del Valle *et al.*'s theory of frequency-resolved photon correlations [37] to compute exactly this measurable property, with no intermediate artificial modes and, therefore, taking into account all the possible interferences and indistinguishability imposed by quantum mechanics. This theory establishes that frequency-resolved correlations of the light emitted by any open quantum-system are the same as the correlations between "sensors" at these frequencies. These sensors are commuting modes with number operator n_i, $i = 1, 2$, and decay rate Γ that are weakly coupled to the system with a constant ε. Frequency-resolved correlations are then computed as:

$$g_\Gamma^{(2)}(\omega_1,\omega_2) = \lim_{\varepsilon\to 0} \frac{\langle n_1 n_2\rangle}{\langle n_1\rangle\langle n_2\rangle}\,. \tag{3}$$

With such a theoretical apparatus, a full mapping of the photon correlations can be obtained. For the case of the Mollow triplet that we have chosen for illustration, the problem takes the vivid form pictured in Fig. 1. The spectral shape—the triplet—is represented in log scale with a choice of five frequency windows, centered at $\pm\omega_T$ (tails), $\pm\omega_S$ (sidebands) and ω_C (central peak). A quantum Monte Carlo trajectory was calculated to simulate the photon-detection events [38] for photo-detectors measuring in these windows. The emitted photons in a small fraction of the trajectory are represented with ticks on the projected plane of Fig. 1(a). The intensities vary in each frequency window: there is of course more signal in the central peak than in the sidebands and more so than in the tails. What is of interest to the quantum optician is the statistical distribution of, and the correlation between, these photons. The autocorrelation in a given window gives the statistics of emission. While the light emitted by the two-level system

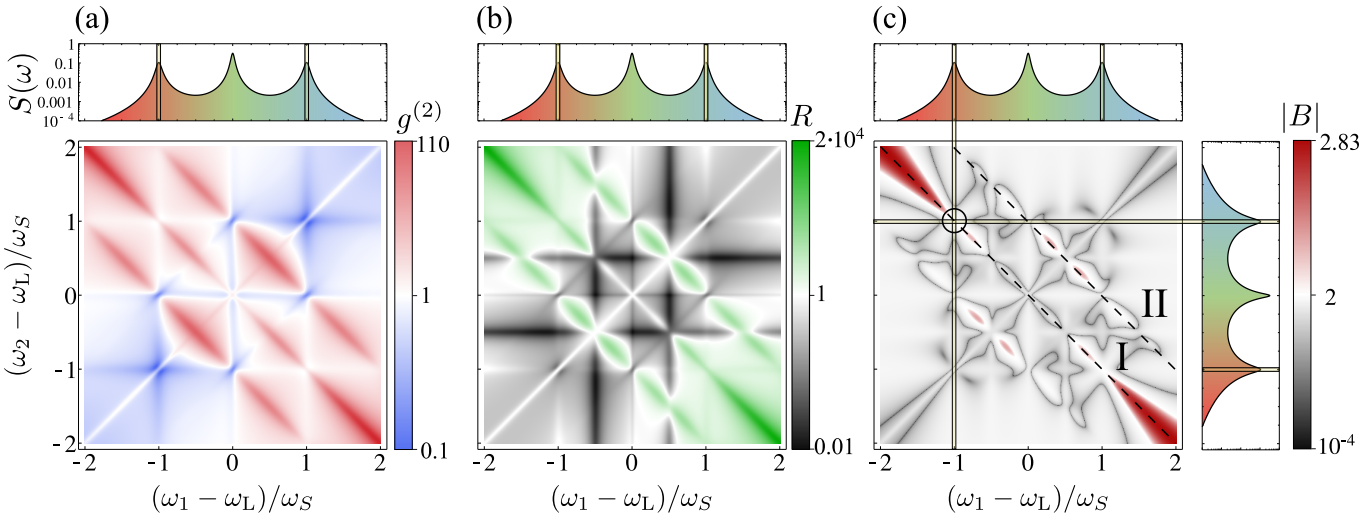

FIG. 2: Landscapes of correlations in the frequency domain: (a) $g_\Gamma^{(2)}(\omega_1,\omega_2)$, (b) $R_\Gamma(\omega_1,\omega_2)$ and (c) $B_\Gamma(\omega_1,\omega_2)$. In (b) [resp. (c)], the color code is such that green [resp. red] violates the CSI [resp. BI] and thus corresponds to genuine quantum correlations between the detected photons in the corresponding energy windows, while black and white do not (with white maximizing the inequality). The violation originates from the emission that involve virtual states. Dashed lines in (c) are the cuts in Fig. 3(a). The spectra on the axes show which frequency windows are correlated. Parameters are the same as in Fig. 1. The evolution of these landscapes as a function of the detector linewidth is provided in the supplementary material.

overall is perfectly antibunched, one sees that by spectral filtering, one can "distill" light with different statistical properties [39], namely, i) uncorrelated in the tails, ii) antibunched in the satellite peaks and iii) bunched in the central peak. One can similarly calculate the cross-correlations between photons from two different windows, showing this time that photons from the satellites are positively correlated, $g_\Gamma^{(2)}(-\omega_S,\omega_S)\approx 1.5$, while photons from one satellite and the central peak are anti-correlated, with $g_\Gamma^{(2)}(\omega_C,\omega_S)\approx 0.23$. It is worth noting here that the stronger correlations come from the tail events, with $g_\Gamma^{(2)}(-\omega_T,\omega_T)\approx 14$ for the window chosen, and increasing with greater still separations. The price to pay for these strong correlations is a correspondingly vanishing signal. Events are more rare but the strength of their correlations is increased. This is a general trend.

At this point, we have set the stage to fully characterize the quantumness of the emission in terms of violation of the CSI and BI. This requires simply to substitute $g_{12}^{(2)}$ in Eq. (1) by $g_\Gamma^{(2)}(\omega_1,\omega_2)$ and correlators $\langle a_i^\dagger a_j^\dagger a_j a_i\rangle$ by $\langle n_i n_j\rangle$ in Eq. (2) and span over all the frequencies. Note the considerable improvement as compared to the mode-correlation approach, since a continuum of frequencies in windows of arbitrary sizes can now be investigated without assumptions on the order of emission. Figure 2 shows three correlation landscapes in the frequency domain depicting the value of $g_\Gamma^{(2)}(\omega_1,\omega_2)$, $R_\Gamma(\omega_1,\omega_2)$ and $B_\Gamma(\omega_1,\omega_2)$ for the same configuration. It immediately comes across that the quantum character of the emission, where the inequalities are violated, is structured along three antidiagonals. These correspond to two-photon emission in a "leapfrog process" [40] that jumps over the intermediate real state by involving a virtual state instead. The antidiagonal, line I, corresponds to transitions from $|+\rangle$ to $|+\rangle$ two rungs below (or $|-\rangle$ to $|-\rangle$), as is sketched in Fig. 1(b), thus satisfying $\omega_1+\omega_2=0$. Line II and its symmetric correspond to transitions from $|+\rangle$ to $|-\rangle$ and from $|-\rangle$ to $|+\rangle$ respectively, satisfying $\omega_1+\omega_2=\pm\omega_S$. The CSI and BI are less, or are not, violated whenever the intermediate rung intersects a real state, as seen by the fact that the green and red patches are depleted or pierced when intersecting the sidebands $\pm\omega_S$. This is particularly important since previous studies focused precisely on correlations between real transitions, i.e., between peaks, such as indicated by the scope in Fig. 2(c). Instead, the exact treatment shows that these are detrimental to the effect, that is optimum when involving virtual states, since these are the vector of quantum correlations. One can prove [44] that a single-mode emitter with no dressing (here by the laser) never violates the CSI or BI, regardless of frequencies and detection widths. Notably, this is true even if the emitter is a two-level system and exhibits perfect antibunching, $g^{(2)}(\tau=0)=0$, which is a CSI violation in time [41]. All this evidence confirms that CSI and BI violations are rooted in the quantum dynamics that involves a virtual state in a collective de-excitation in the quantum ladder of the dressed states.

A quantitative reading of these results is given in Fig. 3. In panel (a), slices in the landscape are shown along lines I and II (cf. Fig. 2(c)). The quantum correlations violating the CSI are found in the side peaks and beyond, being larger the farther from the peaks. The

same feature is present in the BI violation, which furthermore tends to the maximum value allowed $B = 2\sqrt{2}$.

The two lower figures of panel (a) show $g_\Gamma^{(2)}(\omega,\omega)$ and $g_\Gamma^{(2)}(\omega,-\omega)$—that can be used to compute both R and B along line I—as calculated exactly (solid red lines) [37, 40] and through the auxiliary multi-mode approximation used in previous works (dashed blue) [29, 30]. In the latter case, the estimation is local around the peaks, that is, at $\omega/\omega_S = \pm 1$ and 0 (dotted vertical lines), where it is seen to be fairly accurate indeed, although not numerically exact. It can still lead to qualitative error, e.g., the autocorrelation at the sidebands is exactly zero in this approximation, predicting arbitrary violation of the CSI even when it is obeyed and an unphysical violation of the BI [45]. Furthermore, these expressions are found in limiting cases for the filter linewidths $\Gamma \ll \gamma_\sigma \ll \Omega$ and $\gamma_\sigma \ll \Gamma \ll \Omega$. Both assume that the peaks are well separated, to allow for the multiple-mode approximation. They predict no CSI or BI violation for narrow filters, which is ultimately verified although for values of the detector linewidth so small that they are unphysical. The solid lines in Fig. 3(b) show the dependence of R_Γ and B_Γ on the detector linewidth Γ for the three sets of frequencies on line I depicted in Fig. 3(c). The corresponding dependence on the full landscape of correlations is provided in the supplementary material. For the already extremely small value of frequency windows $\Gamma = 0.1\gamma_\sigma$, the CSI and BI can be violated, in contradiction with the prediction of the multiple-mode approximation. There are mainly three regimes of frequency correlations: narrow filters, peaks filtering and overlapping windows. While narrow filters better define the structure, they also correspond to longer times of integration due to the time-frequency uncertainty and thus average out the correlations. A maximum is found when filtering in windows of the order of the peak linewidth or above, which is a welcomed result for an experimentalist. The overlap of the filters marks a change of trend in all the curves, due to a competition between various phenomena involving, for instance, various transitions as well as averaging over different types of interferences. The dashed lines in Fig. 3(b) show the value of $\Gamma S_\Gamma(\omega)$ corresponding to the amount of signal that can be collected with a detector of linewidth Γ at the frequency ω [37]. This way, one can easily compare, for a given amount of available signal, the different degrees of violation which are accessible simply by selecting the frequency and the window of the detector appropriately. Since such correlations are useful for technological purposes, the ability to compute the entire landscape of frequency correlations becomes helpful for optimizing quantum information processing. Correlations along line I of the map arise from a well defined family of virtual processes, from which sideband correlations have been shown to be just a particular, and in fact also a detrimental case. By positioning the filters

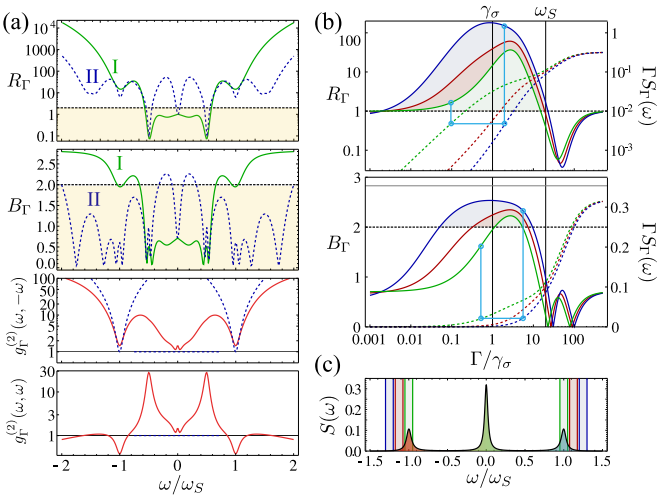

FIG. 3: (a) Cuts of R_Γ (top panel) and B_Γ (second panel) along the lines I and II of Fig. 2(c), together with the corresponding photon-correlation $g_\Gamma^{(2)}(\omega,\pm\omega)$ computed exactly (solid red) or through the multiple-mode approximation (dashed blue). In the lower panel, the absence of the latter curve in some domains correspond to values which are exactly zero. (b) Solid lines: R_Γ (top panel) and B_Γ (bottom panel) as a function of the detector linewidth for the three frequencies depicted in panel (c). Dashed lines: Amount of signal $\Gamma S_\Gamma(\omega)$ that can be collected for the corresponding filter linewidth. Blue points illustrate how two configurations with the same amount of collected signal can yield different degrees of violation. (c) Resonance fluorescence spectrum, this time in linear scale, displaying the characteristic Mollow triplet and three sensors with linewidth $\Gamma = 2\gamma_\sigma$ centred at the frequencies used for panel (b): ω_S, $1.125\,\omega_S$ and $1.25\,\omega_S$. Parameters are the same as in Fig. 1.

away from the sidebands and increasing the frequency window of detection, it is possible to distill light showing stronger quantum correlations without paying any price on the signal.

In conclusion, we have shown how to evidence and optimize CSI and BI violations between photons resolved in frequency from a quantum source, with no constrains nor approximations from the theoretical description. Maximum violation is to be found not when correlating peaks in the spectrum, as previously thought, and thus linked to transitions between real states, but when involving virtual processes in the quantum dynamics. These results show the potential of frequency correlations to engineer quantum correlations, and could be applied towards the design of optimum quantum information processing devices.

We acknowledge the IEF project SQUIRREL (623708), the Spanish MINECO (MAT2011-22997, FPI & RyC programs), the CAM (S2009/ESP-1503) and the ERC PolaFlow.

* Electronic address: fabrice.laussy@gmail.com

[1] R. Loudon, Rep. Prog. Phys. **43**, 913 (1980).
[2] J. S. Bell, Rev. Mod. Phys. **38**, 447 (1966).
[3] M. D. Reid and D. F. Walls, Phys. Rev. A **34**, 1260 (1986).
[4] G. Hardy, J. Littlewood, and G. Pólya, *Inequalities* (Cambridge Mathematical Library, 1952), 2nd ed.
[5] A. K. Ekert, Phys. Rev. Lett. **67**, 661 (1991).
[6] R. J. Glauber, Phys. Rev. **130**, 2529 (1963).
[7] N. A. Ansari, Phys. Rev. A **55**, 1639 (1997).
[8] J. F. Clauser, Phys. Rev. D **9**, 853 (1974).
[9] A. Aspect, P. Grangier, and G. Roger, Phys. Rev. Lett. **47**, 460 (1981).
[10] A. Aspect, J. Dalibard, and G. Roger, Phys. Rev. Lett. **49**, 1804 (1982).
[11] A. Aspect, P. Grangier, and G. Roger, Phys. Rev. Lett. **49**, 91 (1982).
[12] M. A. Rowe, D. Kielpinski, V. Meyer, C. A. Sackett, W. M. Itano, C. Monroe, and D. J. Wineland, Nature **409**, 791 (2001).
[13] A. Kuzmich, W. P. Bowen, A. D. Boozer, A. Boca, C. W. Chou, L.-M. Duan, and H. J. Kimble, Nature **423**, 731 (2003).
[14] V. Balić, D. A. Braje, P. Kolchin, G. Y. Yin, and S. E. Harris, Phys. Rev. Lett. **94**, 183601 (2005).
[15] J. K. Thompson, J. Simon, H. Loh, and V. Vuletić, Science **313**, 74 (2006).
[16] H. Sakai, T. Saito, T. Ikeda, K. Itoh, T. Kawabata, H. Kuboki, Y. Maeda, N. Matsui, C. Rangacharyulu, M. Sasano, et al., Phys. Rev. Lett. **97**, 150405 (2006).
[17] A. M. Marino, V. Boyer, and P. D. Lett, Phys. Rev. Lett. **100**, 233601 (2008).
[18] K. V. Kheruntsyan, J.-C. Jaskula, P. Deuar, M. Bonneau, G. B. Partridge, J. Ruaudel, R. Lopes, D. Boiron, and C. I. Westbrook, Phys. Rev. Lett. **108**, 260401 (2012).
[19] Q.-F. Chen, B.-S. Shi, M. Feng, Y.-S. Zhang, and G.-C. Guo, Opt. Express **16**, 21708 (2008).
[20] S. Du, P. Kolchin, C. Belthangady, G. Y. Yin, and S. E. Harris, Phys. Rev. Lett. **100**, 183603 (2008).
[21] B. Srivathsan, G. K. Gulati, B. Chng, G. Maslennikov, D. Matsukevich, and C. Kurtsiefer, Phys. Rev. Lett. **111**, 123602 (2013).
[22] H. J. Kimble and L. Mandel, Phys. Rev. A **13**, 2123 (1976).
[23] E. B. Flagg, A. Muller, J. W. Robertson, S. Founta, D. G. Deppe, M. Xiao, W. Ma, G. J. Salamo, and C. K. Shih, Nat. Phys. **5**, 203 (2009).
[24] O. Astafiev, A. M. Zagoskin, A. A. A. Jr., Y. A. Pashkin, T. Yamamoto, K. Inomata, Y. Nakamura, and J. S. Tsai, Science **327**, 840 (2010).
[25] P. Lodahl, S. Mahmoodian, and S. Stobbe, arXiv:1312.1079 (2013), URL `http://arxiv.org/abs/1312.1079`.
[26] B. R. Mollow, Phys. Rev. **188**, 1969 (1969).
[27] C. Cohen-Tannoudji and S. Reynaud, Phil. Trans. R. Soc. Lond. A **293**, 223 (1979).
[28] P. A. Apanasevich and S. Y. Kilin, J. Phys. B.: At. Mol. Phys. **12**, L83 (1979).
[29] C. A. Schrama, G. Nienhuis, H. A. Dijkerman, C. Steijsiger, and H. G. M. Heideman, Phys. Rev. A **45**, 8045 (1992).
[30] G. Nienhuis, Phys. Rev. A **47**, 510 (1993).
[31] A. Aspect, G. Roger, S. Reynaud, J. Dalibard, and C. Cohen-Tannoudji, Phys. Rev. Lett. **45**, 617 (1980).
[32] A. Ulhaq, S. Weiler, S. M. Ulrich, R. Roßbach, M. Jetter, and P. Michler, Nat. Photon. **6**, 238 (2012).
[33] H.-P. Breuer and F. Petruccione, *The Theory of Open Quantum Systems* (Oxford University Press, 2002).
[34] G. W. Gardiner and P. Zoller, *Quantum Noise* (Springer-Verlag, Berlin, 2000), 2nd ed.
[35] L. Knöll and G. Weber, J. Phys. B.: At. Mol. Phys. **19**, 2817 (1986).
[36] J. D. Cresser, J. Phys. B.: At. Mol. Phys. **20**, 4915 (1987).
[37] E. del Valle, A. Gonzalez-Tudela, F. P. Laussy, C. Tejedor, and M. J. Hartmann, Phys. Rev. Lett. **109**, 183601 (2012).
[38] M. B. Plenio and P. L. Knight, Rev. Mod. Phys. **70**, 101 (1998).
[39] E. del Valle, New J. Phys. **15**, 025019 (2013).
[40] A. Gonzalez-Tudela, F. P. Laussy, C. Tejedor, M. J. Hartmann, and E. del Valle, New J. Phys. **15**, 033036 (2013).
[41] R. Loudon, *The quantum theory of light* (Oxford Science Publications, 2000), 3rd ed.
[42] A. Joshi, R. R. Puri, and S. V. Lawande, Phys. Rev. A **44**, 717 (1991).
[43] A term $-(\langle {a_1^\dagger}^2 {a_2}^2\rangle + \langle {a_2^\dagger}^2 {a_1}^2\rangle)$ in the numerator of B is ignored in Ref. [7]. It can be neglected as long as there are not second-order transfer of photons between the modes, but can be important in some configurations. We have verified that this term is indeed negligible in our case.
[44] This can be shown analytically, from the closed form expression Eqs. (6–8) in Ref. [40].
[45] A violation of the Bell's inequality in this condition was predicted by Joshi *et. al.* [42]. However, the violation was considered ill-defined due to the perfect antibunching of the sidebands, emerging as a consequence of the multimode approximation.